

RSC Advances



This is an *Accepted Manuscript*, which has been through the Royal Society of Chemistry peer review process and has been accepted for publication.

Accepted Manuscripts are published online shortly after acceptance, before technical editing, formatting and proof reading. Using this free service, authors can make their results available to the community, in citable form, before we publish the edited article. This *Accepted Manuscript* will be replaced by the edited, formatted and paginated article as soon as this is available.

You can find more information about *Accepted Manuscripts* in the [Information for Authors](#).

Please note that technical editing may introduce minor changes to the text and/or graphics, which may alter content. The journal's standard [Terms & Conditions](#) and the [Ethical guidelines](#) still apply. In no event shall the Royal Society of Chemistry be held responsible for any errors or omissions in this *Accepted Manuscript* or any consequences arising from the use of any information it contains.



Journal Name

COMMUNICATION

An Acentric 3-D Metal-Organic Framework with Threefold Interpenetrated Diamondoid Network: Second-Harmonic-Generation Response, Potential Ferroelectric Property and Photoluminescence†

Received 00th January 20xx,
Accepted 00th January 20xx

DOI: 10.1039/x0xx00000x

www.rsc.org/

Wei-Wei Zhou,^a Bo Wei,^b Feng-Wu Wang,^a Wen-Yan Fang,^a Dao-Fu Liu,^a Yi-Jun Wei,^a Mai Xu,^a Xing Zhao^a and Wang Zhao^{*a}

An excellent one-center-Acceptor-Donor ligand, 2-aminoisonicotinic acid, was successfully employed to obtain an acentric 3-D metal-organic framework, which exhibits unique threefold interpenetrated diamondoid network, second-harmonic-generation response, potential ferroelectric behaviors and photoluminescence.

The development of nonlinear optical (NLO) and ferroelectric materials have recently aroused considerable interest owing to their potential applications in optical signal processing, new laser sources, ferroelectric random access memories, ferroelectric field-effect transistors and so on.¹ To our knowledge, an efficient approach to gain NLO and ferroelectric materials is to synthesize acentric diamondoid networks.² For functional metal-organic frameworks (MOFs), skillful selection of unsymmetrical bridging ligands, which possess push-pull effects and suitable length, could facilitate the construction of *odd*-number interpenetrating diamondoid networks and avoid the introduction of inversion centers.³ In the structure of 2-aminoisonicotinic acid (HL2), electron-donating amino group interacts with electron-withdrawing nitro group via conjugated π -electron reservoir, resulting in push-pull effect. Therefore, HL2 is an excellent one-center-A(acceptor)-D(donor) chromophore and a promising candidate for the design of NLO and ferroelectric MOFs.

Photoluminescence (PL) is another focus of attention for researchers, due to its potential applications in sensing and lighting.⁴ Functional MOFs is an important way for preparation of PL materials. Through tailoring of activated ions and/or organic ligands, various PL materials, even tunable PL

materials, could be gained.⁵ As part of our ongoing efforts to design and synthesize functional MOFs, we select the bridging HL2 ligands as sources to construct a novel Cd(II) compound $[\text{Cd}(\text{C}_6\text{H}_5\text{N}_2\text{O}_2)_2]_{3n} \cdot 4n\text{H}_2\text{O}$ (**1**). Herein, we report the synthesis, structure, topologic network, optical (NLO and PL) and potential ferroelectric properties, dielectric properties and electronic structure of **1**.

Colorless crystals of **1** were attained by reacting $\text{Cd}(\text{CH}_3\text{COO})_2 \cdot 2\text{H}_2\text{O}$ and HL2 under the solvothermal reaction conditions (ESI†). The single-crystal structure of **1** was revealed by single-crystal X-ray diffraction analysis (ESI†), and was further confirmed by satisfactory elemental analysis (ESI†), IR (Fig. S1†) and thermogravimetric analysis (TGA) (Fig. S2†). The simulated and experimental powder X-ray diffraction (XRD) patterns accord with each other well, indicating the phase purity of the product (Fig. S3†). The PXRD (50–300 °C) and TGA indicating that the framework structure of **1** can be retained up to 300 °C. Compound **1** crystallizes in the hexagonal system with noncentrosymmetric space group *R3c*. The asymmetric

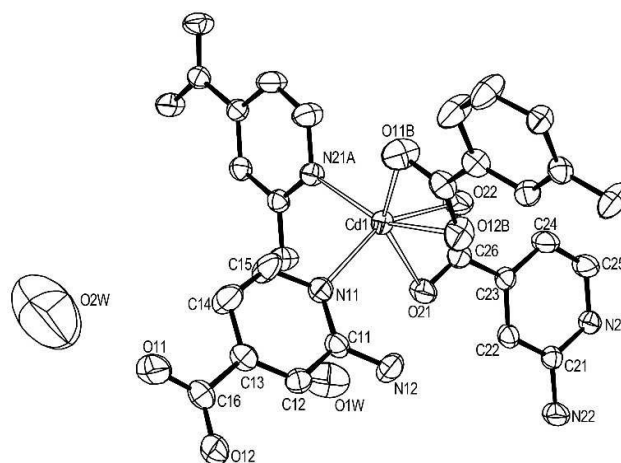


Fig. 1 ORTEP drawing of **1** with 50% thermal ellipsoids with hydrogen atoms being omitted for clarity. (Symmetry codes: A: $-1/3 + x, 1/3 + x - y, -1/6 + z$; B: $x, x - y, 1/2 + z$).

^a Anhui Key Laboratory of Low Temperature Co-fired Materials, College of Chemistry & Materials Engineering, Huainan Normal University, Huainan, Anhui 232038, PR China. E-mail: wzhao@hnnu.edu.cn; Tel: +86 5546862556.

^b School of Chemistry and Materials Engineering, Jiangsu Key Laboratory of Advanced Functional Materials, Changshu Institute of Technology, Changshu, Jiangsu 215500, PR China.

† Electronic Supplementary Information (ESI) available: Experimental details, figures showing IR spectrum, TGA data, X-ray powder diffraction patterns, structural details, diffuse reflection spectra, detailed PL spectra of **1**, HL2, $[\text{Cd}_3(\text{SO}_4)_2(\text{H}_2\text{O})_4]_n$ and HL, band structure, tables for crystallographic data. See DOI: xxx.

unit of **1** contains one Cadmium atom, two deprotonated L²⁻ ligands, one O1W and one-third O2W water molecules (Fig. 1). The Cd1 atom is surrounded by four oxygen atoms (O11, O12, O21, O22) from two different L²⁻ ligands, and two nitrogen atoms (N11, N21) from the others two different L²⁻ ligands, forming a six-coordination geometry. The Cd–O distances vary between 2.305(3)–2.439(3) Å and the Cd–N distances are in the range 2.259(3) and 2.304(3) Å. Thus, each L²⁻ ligand chelates to one Cadmium atom via its carboxyl group and links to another Cadmium atom by its nitrogen atom of pyridine ring, acting as a μ_2 -bridge. These bonding modes make the N21–Cd1–O11 angle 100.67(11)°, N11–Cd1–N21 angle 98.32(11)° and O21–Cd1–N11 angle 91.48(11)°, with a dihedral angle between the plane defined by O11, Cd1, O12 atoms and the plane defined by O11, Cd1, O12 atoms, of approximately 87.389° for compound **1**.

In this manner, each Cadmium atom connects to four neighboring L²⁻ ligands in four directions (Fig. 1), generating a four-connecting node. The L²⁻ ligands function as extended bridges, linking two neighboring Cd centers. Such a connectivity pattern is repeated infinitely to construct the infinite 4-connected net of **1**. And we can find identical adamantanoid cages in the net. A single cage is illustrated in Fig. 2(a), it exhibits Cd···Cd edges which are 9.1963(3) or 9.2147(3) Å long, and the Cd···Cd···Cd angles which range from 91.684 to 126.649°. The maximal dimensions of the cage (corresponding to longest intra-cage Cd···Cd distances) is $a \times 2/3b \times c$ (i.e., 24.06 × 16.04 × 13.22 Å³). Such large cavities induce unusual 3-fold interpenetration of the networks, and

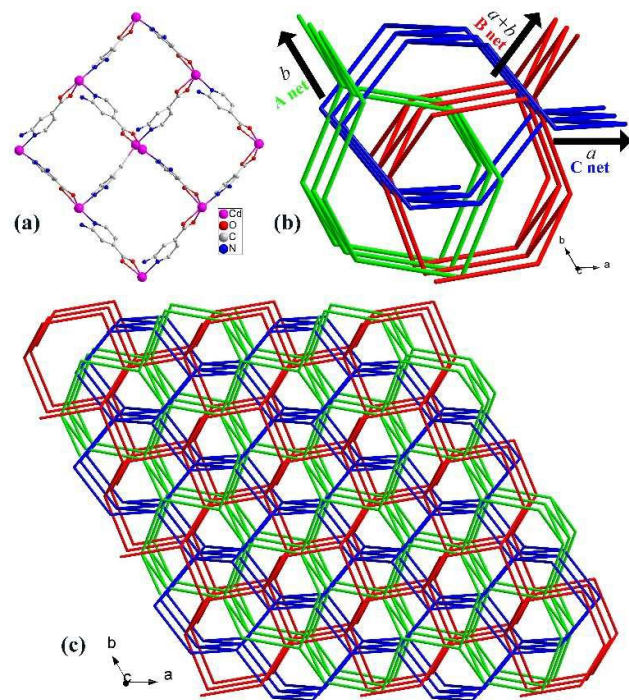


Fig. 2 (a) An adamantanoid cage in **1**; (b) A schematic view of the [1 + 1 + 1] interpenetrating mode of diamondoid network; (c) A schematic view of the threefold diamondoid network of **1**.

the overall topology can be described as a four-connected diamondoid network net with 6⁶ topology (vertex symbol is 6²·6²·6²·6²·6²·6²) (Figure 2). As shown in Fig. 2(b, c) and Fig. S4, there are three nets (A, B and C) in the networks of **1**. Of particular interest, the translation interpenetration vectors of A, B and C nets are different, being [010], [110] and [100], respectively. Therefore, this kind of interpenetration is rototranslational equivalent, we call this a [1 + 1 + 1] interpenetrating diamondoid system. To our knowledge, most of the reported diamondoid-compound nets⁶ are generated by a unique interpenetration vector. Only a few examples, such as {[CuL₂]PF₆]_∞ (HL = 2,7-diazapyrene)⁷, Zn(ain)₂·(DMA) (Hain = 2-aminoisonicotinic acid)⁸ and Cd^{II}Cu^I₂(pybz)₄ (Hpybz = 4-(pyridin-4-yl)benzoic acid)⁹, adopt multidirectional-vectors interpenetrations. In comparison with the known dia-net complexes, the novel interpenetration mode of **1** may be due to the bridging mode of L²⁻ ligands and the crystal symmetry of **1**. In spite of the threefold interpenetration, the whole architecture of **1** still has a solvent-accessible volume of approximately 730.7 Å³ per unit cell (11.0%). In addition, reports on the complexes containing HL₂ or L²⁻ ligands have not been seen so far, compound **1** is the first coordination compound of 2-aminoisonicotinic acid ligand. The whole topological and structural characteristics lead **1** to be an excellent candidate for structural chemistry.

Due to that compound **1** crystallizes in the acentric space group (R3c) which belongs to C_{3v}, one of 10 polar point groups (C₁, C₂, C_s, C_{2v}, C₄, C_{4v}, C₃, C_{3v}, C₆, C_{6v}), compound **1** should have potential NLO and ferroelectric properties. Powder sample of **1** is SHG active with a signal of 0.1 times that of KDP. Moreover, the electric hysteresis loop (Fig. 3(a)) reveals the ferroelectric behavior of **1**. The curve of loop presents a remnant polarization (P_r) of ca. 6.64 nC·cm⁻² and a coercive field (E_c) of ca. 8.45 kV cm⁻¹. The value of spontaneous polarization (P_s) of **1** (ca. 24.00 nC·cm⁻²) is comparable to the value found in the compound [Cd(trtr)₂]_n (Htrtr = 3-(1,2,4-triazole-4-yl)-1H-1,2,4-triazole).¹⁰ In our opinion, the SHE and ferroelectric properties can be attributed to L²⁻ ligands and the unique threefold interpenetration dia network of **1**. The push-pull effect of L²⁻ ligands plays an important role in the enhancement of the dipolar moment.¹¹ Moreover, for the A net of **1**, the orderly arrangement of the organic moieties leads to the generation of its total dipole moment (dipole moment A) (Fig. S5[†]). The angle between vector of dipole moment A and c axis is 141.77°. A plane could be draw through dipole moment A and c axis, and the dihedral angle between it and ac plane is 30° (Fig. S6[†]). In the same way, for dipole moment B (of B net), the angle between its vector and c axis is 141.77°, and the dihedral angle is 30°, too (Fig. S7[†] and S8[†]). And for dipole moment C (of C net), the angle between its vector and c axis is 141.77°, and the dihedral angle is 90° (Fig. S9[†] and S10[†]). The spatial locations of dipole moment A, B and C contribute to a total dipole moment along the c-direction (Fig. S11[†]), and thus strengthen the hyperpolarizability of **1**, which accounts for the SHG response and ferroelectric behaviors.¹²

Figures (Fig. 3(b) and S12[†]) presents the dependence of the dielectric constant (ε') and dielectric loss tangent (tanδ) of

1 on the temperature and frequency. The value of ϵ' is 7.84 at 30 °C and 10 Hz, being much higher than that of compound [Cd(anp)₂Br₂] \cdot H₂O (anp = 2-amino-5-nitropyridine) (0.179, at 10 Hz, 30 °C).¹² The temperature of maximum (T_{\max}) dielectric constant (94.5 °C at 10 Hz) for **1** demonstrated is slightly lower than that of the compound [Cd(anp)₂Br₂] \cdot H₂O (138 °C). And the location of the dielectric constant peaks mainly remains unchanged with variable frequencies, while the T_{\max} of dielectric loss tangent shifts to higher temperatures as frequency decreases (e.g., from T_{\max} = 89.5 °C at 100 kHz to 154.5 °C at 1 Hz).

Intense absorption bands in the UV (200–400 nm) range can be found in reflectance diffusion spectrum of **1**, together with some absorption in the infrared region (1300–2600 nm) (Fig. S13[†]), demonstrating an optical gap of 3.180 eV (Fig. S14[†]). In this work, compound **1** shows a broad emission in the range of 440–600 nm when excited at 424 nm at room temperature (Fig. 4). Compared to the free ligand HL2 (emission at 482 nm with λ_{ex} = 425 nm) (Fig. 4), the emission

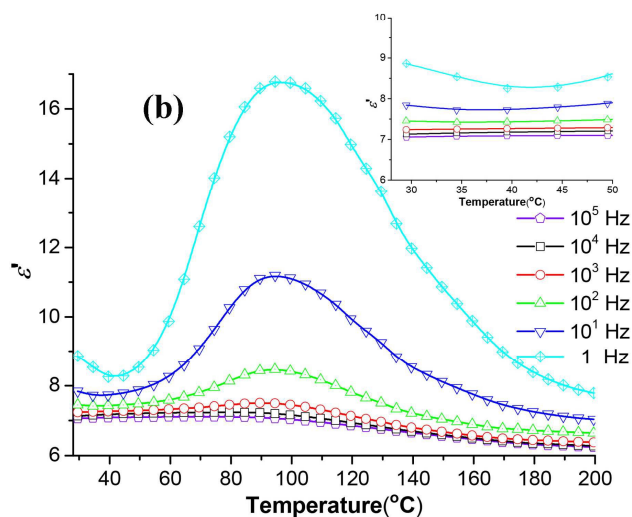
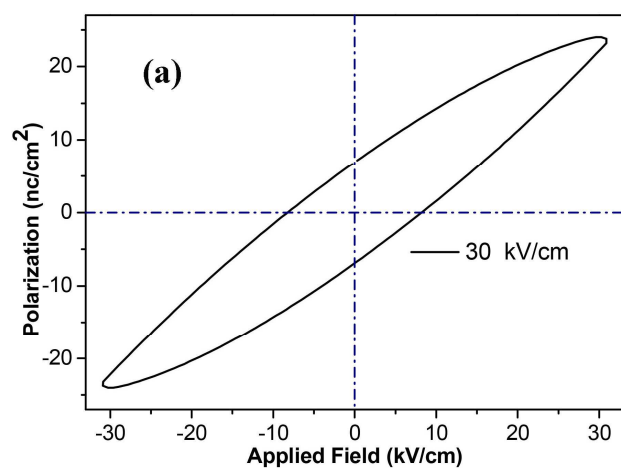


Fig. 3 (a) Electric hysteresis loop of a pellet obtained from a powder sample of **1**; (b) The temperature dependence of the dielectric constant for **1** at various frequencies. The inset shows the enlarged profile ranging from 29 to 50 °C.

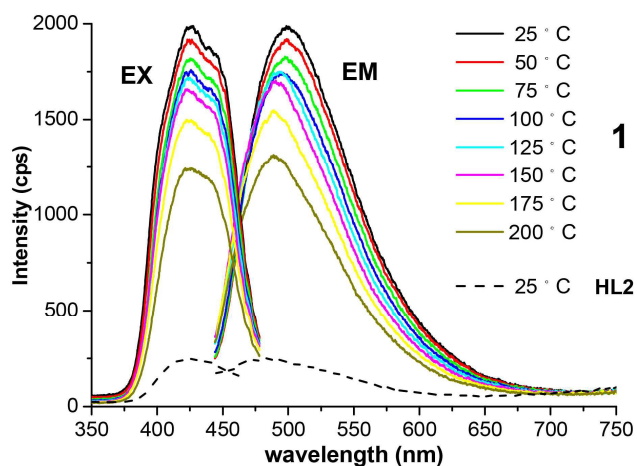


Fig. 4 Solid-state emission and excitation spectra of **1** (the temperature dependence) and HL2 (at room temperature) under the same conditions.

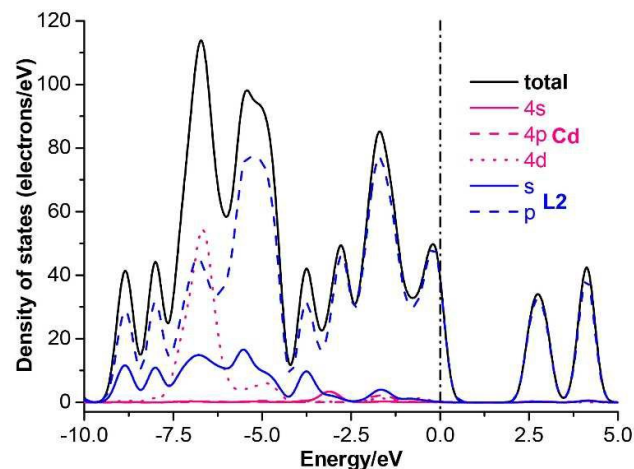


Fig. 5 The total and partial DOS of **1**. The position of the Fermi level is set at 0 eV.

peak of **1** displays small red-shift of 16 nm and enhanced PL intensity. The internal quantum yield of **1** is 22.45% when excited by 424 nm light (Fig. S15[†]), and the internal quantum yield of HL2 is 5.71% when excited by 425 nm light (Fig. S16[†]). Compound **1** and HL2 are also reflected in the CIE chromaticity coordinates (Fig. S17[†]), which are in the green region with values of (0.25, 0.45) for **1** and (0.26, 0.37) for HL2, respectively. It is worth noting that the broad excitation spectrum of **1** matches well with the emission of the commercial InGaN LED chip (360–470 nm), which indicates that **1** can be used as green-emitting phosphors for white LEDs. Moreover, Fig. 4 also shows the temperature-dependent PL spectra of **1**. The relative peak intensity decreases marginally with rising temperature. It reached 88% of initial value at 100 °C and then 75% at 175 °C. The small decrease in the emission intensity indicates a low thermal quenching. The profiles shown in Fig. 4 allow us tentatively to ascribe the emission of **1** to L2[−] ligand.

In order to better understand the PL **1**, electronic structure of **1** was theoretically calculated (ESI[†]). An indirect band gap of 2.550 eV can be obtained from the theoretical-calculation results of **1** (Fig. S18[†]), which is lower than the experimental value (3.180 eV). This may be due to the inaccurate description of the eigenvalues of the electronic states in generalized gradient approximation (GGA). Fig. 5 presents the total and partial density of states (DOS) of **1**, we find that not only the top of the valence bands (VBs) (from -4.2 to Fermi level (0 eV)) but also the bottom of the conduction bands (CB) (from 2.0 to 5.0 eV) are mainly contributed by p- π orbitals of L²⁻ ligands. From this point of view, a conclusion can be drawn that the emissions of **1** can be mainly attributed to ligand-centered charge transitions based on L²⁻ ligands. This result is consistent with the above tentative ascription for the PL of **1**.

Conclusions

In conclusion, a 3-D acentric Cd(II) MOF (**1**) based on 2-aminoisonicotinic acid, has been prepared via solvothermal reaction. Compound **1** contains adamantanoid cages, and exhibits unique 3-fold interpenetrated diamondoid network. Especially, the translation interpenetration vectors of three nets are different. Benefiting from the non-centrosymmetric polar packing arrangement and the one-center-A-D ligands, compound **1** displays SHG response and ferroelectric behaviors, indicating its broad potential in the application for NLO and ferroelectric materials. Moreover, PL spectra of **1** demonstrates that **1** can be used as green-emitting phosphors for white LEDs.

Acknowledgements

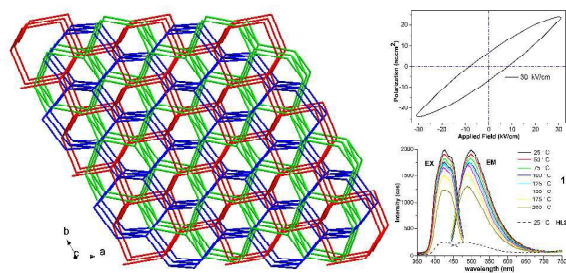
We gratefully acknowledge the financial support of the NSF of China (21201071, 61205213, 21176099), the NSF of Anhui Province (1208085QB42) and of Jiangsu Province (BK2012210), Science and Technology Project of Huainan City (2013A4105), the NSF of Jiangsu Higher Education Institutions of China (10KJB430001), the Opening Fund of Jiangsu Key Laboratory of Advanced Functional Materials (12KFJJ010) and Program for Innovative Research Team in Huainan Normal University.

Notes and references

- (a) C. Chen and G. Liu, *Annu. Rev. Mater. Sci.*, 1986, **16**, 203; (b) D. Burland, *Chem. Rev.*, 1994, **94**, 1; (c) M. Fiebig, V. V. Pavlov and R. V. Pisarev, *J. Opt. Soc. Am. B*, 2005, **22**, 96; (d) W. Zhang, H.-Y. Ye and R.-G. Xiong, *Coord. Chem. Rev.*, 2009, **253**, 2980; (e) E. Cross, *Nature*, 2004, **432**, 24; (f) W. Zhang and R.-G. Xiong, *Chem. Rev.*, 2012, **112**, 1163.
- (a) O. Ermer and A. Eling, *Angew. Chem. Int. Ed. Engl.*, 1988, **27**, 829; (b) O. Ermer, *J. Am. Chem. Soc.*, 1988, **110**, 3747; (c) D. M. Proserpio, R. Hoffmann and P. Preuss, *J. Am. Chem. Soc.*, 1994, **116**, 9634; (d) O. R. Evans and W. Lin, *Acc. Chem. Res.*, 2002, **35**, 511; (e) O. R. Evans and W. Lin, *Chem. Mater.*, 2001, **13**, 2705.

- (a) H.-L. Jiang, T. A. Makal and H.-C. Zhou, *Coord. Chem. Rev.*, 2013, **257**, 2232; (b) I. A. Baburin, V. A. Blatov, L. Carlucci, G. Ciani and D. M. Proserpio, *J. Solid State Chem.*, 2005, **178**, 2452; (c) O. R. Evans, R.-G. Xiong, Z. Wang, G. K. Wong and W. Lin, *Angew. Chem. Int. Ed.*, 1999, **38**, 536.
- (a) A. Y.-Y. Tam, K. M.-C. Wong and V. W.-W. Yam, *J. Am. Chem. Soc.*, 2009, **131**, 6253; (b) K. Jayaramulu, P. Kanoo, S. J. George and T. K. Maji, *Chem. Commun.*, 2010, **46**, 7906; (c) F. Wang, X. Xue and X. Liu, *Angew. Chem. Int. Ed.*, 2008, **47**, 906; (d) S. Sapra, S. Mayilo, T. A. Klar, A. L. Rogach and J. Feldmann, *Adv. Mater.*, 2007, **19**, 569; (e) W. Zheng, P. Huang, D. Tu, E. Ma, H. Zhu and X. Chen, *Chem. Soc. Rev.*, 2015, **44**, 1379.
- (a) M. D. Allendorf, C. A. Bauer, R. K. Bhakta and R. J. T. Houk, *Chem. Soc. Rev.*, 2009, **38**, 1330; (b) Y. Cui, Y. Yue, G. Qian and B. Chen, *Chem. Rev.*, 2012, **112**, 1126; (c) D. F. Sava Gallis, L. E. S. Rohwer, M. A. Rodriguez and T. M. Nenoff, *Chem. Mater.*, 2014, **26**, 2943; (d) T. Lasanta, M. E. Olmos, A. Laguna, J. M. López-de-Luzuriaga and P. Naumov, *J. Am. Chem. Soc.*, 2011, **133**, 16358; (e) M.-S. Wang, S.-P. Guo, Y. Li, L.-Z. Cai, J.-P. Zou, G. Xu, W.-W. Zhou, F.-K. Zheng and G.-C. Guo, *J. Am. Chem. Soc.*, 2009, **131**, 13572; (f) W.-W. Zhou, W. Zhao, F.-W. Wang, W.-Y. Fang, D.-F. Liu, Y.-J. Wei, M. Xu, X. Zhao and X. Liang, *RSC Adv.*, 2015, **5**, 42616.
- (a) T.-W. Tseng, T.-T. Luo, C.-C. Tsai and K.-L. Lu, *CrystEngComm*, 2015, **17**, 2935; (b) X.-L. Wang, C. Qin, E.-B. Wang, L. Xu, Z.-M. Su and C.-W. Hu, *Angew. Chem. Int. Ed.*, 2004, **43**, 5036; (c) X.-F. Wang, Y.-B. Zhang and Y.-Y. Lin, *CrystEngComm*, 2013, **15**, 3470; (d) F. Wang, Y.-X. Tan, H. Yang, H.-X. Zhang, Y. Kang and J. Zhang, *Chem. Commun.*, 2011, **47**, 5828.
- A. J. Blake, N. R. Champness, A. N. Khlobystov, D. A. Lemenovskii, W.-S. Li and M. Schröder, *Chem. Commun.*, 1997, 1339.
- F. Wang, Y.-X. Tan, H. Yang, Y. Kang and J. Zhang, *Chem. Commun.*, 2012, **48**, 4842.
- Y.-P. He, Y.-X. Tan and J. Zhang, *CrystEngComm*, 2012, **14**, 6359.
- W.-W. Zhou, J.-T. Chen, G. Xu, M.-S. Wang, J.-P. Zou, X.-F. Long, G.-J. Wang, G.-C. Guo and J.-S. Huang, *Chem. Commun.*, 2008, 2762.
- (a) D.-W. Fu, W. Zhang and R.-G. Xiong, *Cryst. Growth Des.*, 2008, **8**, 3461; (b) J.-S. Guo, G. Xu, X.-M. Jiang, M.-J. Zhang, B.-W. Liu and G.-C. Guo, *Inorg. Chem.*, 2014, **53**, 4278.
- W.-W. Zhou, W. Zhao, B. Wei, F.-W. Wang, Y.-H. Chen, W.-Y. Fang and X. Zhao, *Inorg. Chim. Acta*, 2012, **386**, 17.

Graphical Abstract



An solvothermally synthesized acentric 3-D Cd(II) metal-organic framework was found exhibiting unique threefold-interpenetration diamondoid architecture, second-harmonic-generation efficiency, potential ferroelectric property and photoluminescence.